

Este documento es una versión postprint de:

Besharatloo, H., Roa, J.J., Dios, M., Mateo, A.;  
Ferrari, B., Gordo, E., Llanes, L. (2017).  
Micromechanical properties of a Ti(C,N)-FeNiC  
composite: statistical method. *Anales de Mecánica de  
la Fractura*, 34, pp. 494-497.

# MICROMECHANICAL PROPERTIES OF A Ti(C,N)-FeNiC COMPOSITE: STATISTICAL METHOD

H. Besharatloo<sup>1</sup>, J.J.Roa<sup>1,\*</sup>, M. Dios<sup>2</sup>, A. Mateo<sup>1</sup>, B. Ferrari<sup>3</sup>, E. Gordo<sup>2</sup>, L.Llanes<sup>1</sup>

<sup>1</sup>CIEFMA-Departament de Ciència dels Materials i Enginyeria Metal·lúrgica, Universitat Politècnica de Catalunya, Campus Diagonal Besòs (EEBE), C/ d'Eduard Maristany 10-14, 08019 Barcelona, España

<sup>2</sup>GTP-Grupo de Tecnología de Polvos, Universidad Carlos III Madrid, Escuela Politécnica Superior, Av. De la Universidad 30, 28911 Leganés, España

<sup>3</sup>Instituto de Cerámica y Vidrio (ICV-CSIC), C/ Kelsen 5, Campus de Cantoblando. 28049 Madrid, España

\* Persona de contacto: [joan.josep.roa@upc.edu](mailto:joan.josep.roa@upc.edu)

## RESUMEN

Durante los últimos años, se han invertido muchos esfuerzos para diseñar nuevos materiales alternativos a los metales duros (WC-Co), que exhiban respuestas mecánica y tribológica similar a la de éstos. El excelente comportamiento de los compuestos WC-Co se atribuye principalmente a su ensamblaje microestructural, debido a la combinación de dos fases con propiedades muy diferentes a nivel local. En el presente trabajo se pretende evaluar la relación microestructura/propiedades micromecánicas de nuevos materiales compuestos cerámico-metal del sistema Ti(C,N)-Fe,Ni. Para ello se ha utilizado un procedimiento sistemático que consta de varias etapas.

**PALABRAS CLAVE:** Compuestos metal-cerámicos, nanoindentación masiva, análisis estadístico

## ABSTRACT

In recent years, many efforts have been invested to design new alternative materials to substitute hardmetals (WC-Co) that exhibit similar mechanical and tribological response. The outstanding behaviour of WC-Co composites is mainly attributed to its microstructural assemblage, due to the combination of two phases with very different properties at the local level. The present work is aimed to evaluate the microstructure/micromechanical properties of new ceramic-metal Ti(C,N)-Fe,Ni composite systems. A systematic procedure consisting of several stages has been used for this purpose.

**KEYWORDS:** Metallic-ceramic composites, massive nanoindentation, statistical analysis

## 1. INTRODUCTION

The outstanding mechanical properties exhibited by hardmetals (WC-Co system) results from the combination of two phases with quite different properties at the local level. In particular, this is true regarding experimental analysis on the influence of phase nature, crystal orientation and interfacial adhesion strength on hardness for Ti(C,N)-FeNiC composites. The present work aims to conduct a systematic micromechanical study of the mechanical integrity of five Ti(C,N)-FeNiC systems. In doing so, it is attempted by combining massive nanoindentation and statistical analysis, using the methodology proposed by Ulm and co-workers to extract the intrinsic hardness for each constitutive phase.

## 2. EXPERIMENTAL PROCEDURE

### 2.1. Sample preparation

Titanium carbonitride ([Ti(C,N)] grade C, H. C. Stark, Germany), iron (Fe SM, H.C. Stark, Germany) and nickel (Ni 210H, INCO, Canada) submicronic powders were used as commercial starting materials. Particle size and specific surface area of the powders were determined with a laser analyzer (Mastersizer S, Malvern instruments Ltd., UK) and by one point N<sub>2</sub> absorption (Monosorb Surface Area, Quantachrome Corporation, USA), respectively. Density of the as-received powders was measured using a Monosorb Multipycnometer (Quantachrome Corporation, USA). The results are shown in Table 1.

Table 1. Characterization of the as-received powders.

Characteristics		Powder		
		Ti(C,N)	Fe	Ni
Size	D <sub>v50</sub> (µm)	2.1	3.5	1.7
	D <sub>BET</sub> (µm)	0.4	1.2	0.2
	F <sub>ag</sub>	5.0	3.0	10.0
Density (g·cm <sup>-3</sup> )		5.1	7.8	8.9
Surface area (m <sup>2</sup> /g)		3.0	0.6	4.0

From these powders, high solid content suspensions were formulated using water as dispersion media [1]. The suspensions were prepared in deionized water with HTMA to adjust the pH up to 10-11, where surfaces are chemically stable [2,3]. Then 0.4 wt.% of PEI was added as dispersant. Ti(C,N) and Fe/Ni (85/15 wt.%) slurries were prepared separately and milled in a ball mill for 1 h, using Si<sub>3</sub>N<sub>4</sub> and nylon balls, respectively. In order to evaluate the effect of a small addition of carbon, a graphite suspension of 10 g/L was prepared in ethanol using Black Carbon (ISTA, Germany) with a density of 2.24 g·cm<sup>-3</sup> and a mean particle size of 18 μm. After milling, Ti(C,N), Fe/Ni and carbon suspension was mixed to get the desired specimen, see Table 2. Once the suspension was prepared 2 wt.% of polyvinyl alcohol was added as binder [4]. After PVA addition, the suspension remained 20 min under mechanical stirring before it was sprayed.

Table 2. Formulation of the suspensions.

Samples	Vol.%		Composition metal matrix, wt.%		
	Ti(C,N)	Fe/Ni	Fe	Ni	C
15FeNiC	85	15	85	15	+0.5

Stable aqueous suspensions were submitted to spray-dry to obtain agglomerates able to be pressed (SDP route). For this purpose, an atomizer LabPlant SD-05 (North Yorkshire, UK) was used with the main controlled operating parameters being the temperature at the inlet (190 °C) and at the exhaust (100 °C), the slurry pump rate (2 l/h), and the atomizing nozzle design set to provide spherical agglomerates with high compressibility able to be shaped by uniaxial pressing [5]. Subsequently, granules were pressed at 600 MPa in an uniaxial die into cylinders of 16 mm in diameter. Sintering was conducted in high vacuum (10<sup>-5</sup> bar) at 1450 °C for 2 h, with a step of 30 min at 800 °C.

Prior the microstructural and micromechanical characterization, the surfaces were polished with diamond paste down to 3 μm, with a final polishing step with colloidal alumina.

## 2.2. Microstructural characterization

A field emission scanning electron microscopy (FESEM) image of the material investigated is shown in Figure 1.

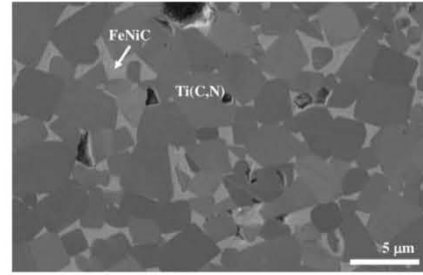


Figure 1. FESEM micrograph of the 15FeNiC microstructure for the cermet grade studied.

Carbide contiguity was assessed from best-fit equations following empirical relationships proposed by Roebuck and Almond [6-9], but extending them to include the influence of carbide size [7,8]. Binder mean free path was finally estimated from the contiguity data [6,9]. The corresponding microstructural parameters are: nominal weight fraction of binder, %vol. FeNiC = 15 %; mean grain size of Ti(N,C),  $d_{Ti(N,C)} = 2.22 \pm 1.14 \mu\text{m}$ , mean free path in binder,  $\lambda_{FeNiC} = 0.76 \pm 0.14 \mu\text{m}$ , and contiguity,  $C_{Ti(N,C)} = 0.47$ .

## 2.3. Nanoindentation process

Mechanical properties of the Ti(C,N)-FeNiC composite included the evaluation of their effective hardness ( $H$ ) through instrumented indentation. Nanoindentation tests were performed on a Nanoindenter XP (MTS), equipped with a continuous stiffness measurement module. The micromechanical characterization was carried out with a Berkovich indenter tip, and experimental data were analysed using the Oliver and Pharr methodology [10,11]. The diamond indenter shape was carefully calibrated with a fused silica standard [10]. Two different steps of experiments were done. The composite mechanical response for the Ti(C,N)-FeNiC specimen was assessed as the average behaviour of 16 imprints, organized in an homogeneous array of 4 by 4, at 2000 nm maximum penetration depth (or until reaching maximum applied load of 650 mN). The distance between imprints was kept constant and equal to 50 μm in order to avoid any overlapping effect. After that, in order to statistically determine the intrinsic hardness for each constitutive phase as well as their anisotropy, three different spaced arrays of 625 imprints (25 by 25, and separated 5 μm from each other) were done at 200 nm of maximum penetration depth, according to the method proposed by Ulm and co-workers [12-15].

## 3. STATISTICAL METHOD

The statistical analysis proposed by Ulm and Constantinides [12-15] is based on the consideration of a sample as composed by several distinct constituent and phases, i.e. ceramic particles, Ti(C,N), and metallic binder, FeNiC, with different mechanical properties. This methodology considers that distribution,  $p_i$ , of the micromechanical properties, in terms of hardness,  $H$ , for

each constituent and phase following a Gaussian distribution:

$$p_i = \frac{1}{\sqrt{2 \cdot \pi \cdot \sigma_i^2}} \cdot \exp\left[-\frac{(H - H_i)^2}{2 \cdot \sigma_i^2}\right] \quad (1)$$

where  $\sigma_i$  is the standard deviation and  $H_i$  the arithmetic mean hardness for each of the number of indentations on the material phases ( $i$ ). The different results are represented by cumulative distribution function, considering that density functions are correctly fitted by Gaussian distribution. In this sense, the experimentally measured intrinsic hardness values may be fitted by using the following expression:

$$CDF = \sum_i^n \frac{1}{2} \cdot f_i \cdot \text{erf}\left[\frac{H - H_i}{\sqrt{2} \cdot \sigma_i}\right] \quad (2)$$

where  $f_i$  is defined as the relative fraction occupied by each constitutive phase. During the deconvolution process, several restrictions were programmed in order to obtain a reliable value. In this regard, the sum of the fraction for each constitutive phase was set at 1, and the fitting process was programmed to be completed when the chi-square was less than  $10^{-15}$ .

## 4. RESULTS AND DISCUSSION

### 4.1. Microstructural parameters

Figure 2 shows the grain size histogram for the Ti(C,N) particles, with a constant bin size of 100 nm, determined from 675 different grains. It mainly presents a bimodal distribution. Peak values at about  $3.1 \mu\text{m}$  and  $1.3 \mu\text{m}$ , are attributed to coarse and fine Ti(C,N) particles, respectively.

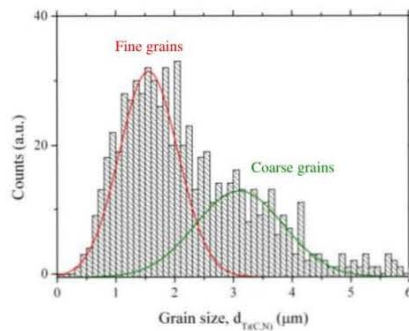


Figure 2. Grain size histogram with 100 MPa of bin size. The simulated fine and coarse distribution are overlapped to the experimental values.

### 4.2. Micromechanical properties

Hardness obtained from Nanoindentation as a function of the displacement into surface is shown in Figure 3. Surface roughness and indenter tip effects on the mechanical response are discerned at very low

penetration depths. Hardness for the Ti(C,N)-FeNiC specimen studied is found to be  $18.0 \pm 0.2 \text{ GPa}$ . Furthermore, FESEM micrograph depicted in Figure 3 (inset) presents the possible damage mechanisms activated during the indentation process around the Berkovich imprint at maximum displacement into surface. As it is evidenced, around the residual imprint several damage events like cracks may be identified (see white arrow).

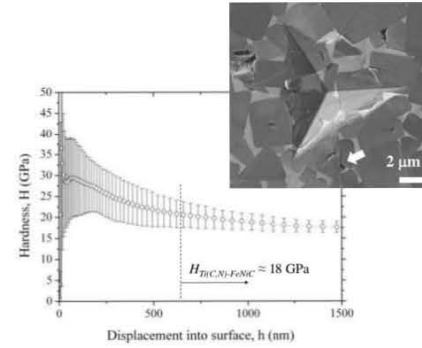


Figure 3. (a) Hardness evolution of Ti(C,N)-FeNiC as a function of the displacement into surface, and (b) residual imprint observed by FESEM.

The hardness histogram, with a constant bin size of 500 MPa, is shown in Figure 4. Three different peaks may be discerned. Two extreme high peak values of around 33 and 24 GPa are attributed to the ceramic phase, while the lowest value peak, centred at 13.9 GPa, is associated with the metallic FeNiC binder phase. The latter is presented here as one of the main outcomes of this research. Within this observation, it is evident that the Ti(C,N) is strongly anisotropic in terms of hardness. Further research may be carried out in order to correlate their intrinsic hardness as a function of their crystallographic orientation.

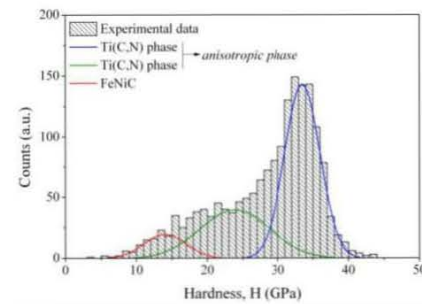


Figure 4. Hardness histogram with 500 MPa of bin size. The simulated hardness using the statistical fitting parameters (summarised in Table 3) are overlap through the statistical method fitting.

As it was mentioned above, in order to obtain a representative distribution of the hardness properties in the heterogeneous composite Ti(C,N)-FeNiC system, a grid of 1875 imprints was performed in the specimen of

interest. Figure 5 corresponds to a FESEM image of a small region of the indentation array.

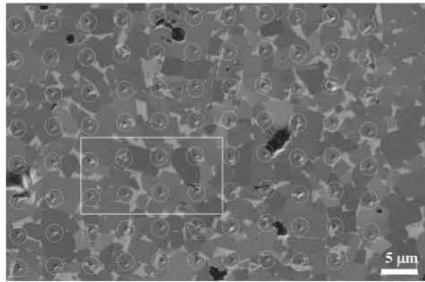


Figure 5. FESEM micrograph image showing one array of indents performed at 200 nm of maximum penetration depth. The distance between imprints has been kept constant to 5  $\mu\text{m}$  in order to avoid any overlapping effect.

Attempting to evaluate whether the penetration depth employed to conduct the massive indentation process is suitable to extract the intrinsic properties for each constitutive phase, magnified FESEM micrograph of a random region (square white region presented in Figure 5) were directly observed, see Figure 6. On the basis of the FESEM observation presented in Figure 6, indentation maximum penetration depth of 200 nm guarantees each indentation test could be treated as an independent statistical event, see \* in Figure 6.

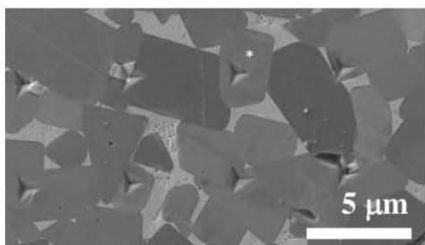


Figure 6. Magnified FESEM image.

## 5. CONCLUSIONS

In this study, experimental and statistical Nanoindentation technique has been implemented for assessment and analysis of the mechanical response of the constitutive phases of Ti(C,N)-FeNiC composite. The main conclusions are as follows:

- Intrinsic hardness values are analysed and determined for the constitutive phases for Ti(C,N)-FeNiC systems, by either different chemical nature or distinct Ti(C,N) orientation.
- Maximum penetration depth of 200 nm, is found to be suitable nanoindentation testing parameters for successful implementation of statistical method in Ti(C,N)-FeNiC systems.
- A clear hardness anisotropy is evidenced for Ti(C,N) crystals. In this regard, hardness for the Ti(C,N) phase is higher than for the metallic FeNiC binder.

## ACKNOWLEDGEMENTS

The currently study was supported by the Spanish Ministerio de Economía y Competitividad through Grant MAT2015-70780-C4-3-P (MINECO/FEDER).

## REFERENCES

- [1] J. A. Escribano, J. I. García, P. Alvaredo, B. Ferrari, E. gordo, A. J. Sanchez-Herencia, Colloidal processing of Fe-based metal ceramic composites with high content of ceramic reinforcement, *Bol. Soc. Esp. Cerámica Vidr.* **52**, 247-250, 2013.
- [2] J. A. Escribano, J. L. García, P. Alvaredo, B. Ferrari, E. Gordo, A. J. Sanchez-Herencia, FGM stainless steel-Ti(C,N) cermets through colloidal processing, *Int. J. Refract. Met. Hard Mater.* **49**, 143-152, 2015.
- [3] P. Parente, A. J. Sanchez-Herencia, M. J. Mesa-Galan, B. Ferrari, Funcionalizing Ti-surfaces through the EPD of hydroxyapatite/Nano  $\text{Y}_2\text{O}_3$ , *J. Phys. Chem. B*, **117**, 1600-1607, 2013.
- [4] R. G. Neves, J. A. Escribano, B. Ferrari, A. J. Sanchez-Herencia, E. Gordo, Improvement of Ti Processing through Colloidal Techniques, *Key Eng. Mater.* **520**, 335-340, 2012.
- [5] R. G. Neves, B. Ferrari, A. J. Sanchez-Herencia, E. Gordo, Colloidal approach for the design of Ti powders sinterable at low temperature, *Mat. Lett.* **107**, 75-78, 2013.
- [6] B. Roebuck, E. A. Almond, Deformation and fracture processes and the physical metallurgy of WC-Co hardmetals, *Int. Mater. Rev.* **33**, 90-110, 1988.
- [7] Y. Torres [Ph.D. thesis], Comportamiento a fractura y fatiga de carburos cementados WC-Co, *Universitat Politècnica de Catalunya*, 2002.
- [8] D. Coureaux [Ph.D. thesis], Comportamiento mecánico de carburos cementados WC-Co: influencia de la microestructura en la resistencia a la fractura, la sensibilidad a la fatiga y la tolerancia al daño inducido bajo solicitaciones de contacto, *Universitat Politècnica de Catalunya*, 2012.
- [9] H. E. Exner, Physical and chemical nature of cemented carbides, *Int. Met. Rev.* **4**, 1149-1173, 1979.
- [10] W. C. Oliver, G. M. Pharr, An improvement technique for determining hardness and elastic modulus using load and displacement sensing indentation experiments, *J. Mater. Res.* **7**, 1564-1580, 1992.
- [11] W. C. Oliver, G. M. Pharr, Measurement of hardness and elastic modulus by instrumented indentation: Advances in understanding and refinements to methodology, *J. Mater. Res.* **19**, 3-20, 2004.
- [12] Constantinides G, Ulm F-J, Van Vliet K. On the use of nanoindentation for cementitious materials. *Mater Struct* 2003;36:191-6.
- [13] Constantinides G, Chandran KSR, Ulm F-J, Van Vliet K. Grid indentation analysis of composite

microstructure and mechanics: principles and validation. *Mater Sci Eng A* 2006;A430:189–202.

[14] Constantinides G, Ulm F-J. The nanogranular nature of C S H. *J Mech Phys Solids* 2006;55:64–90.

[15] Ulm F-J, Vandamme M, Bobko C, Ortega JA, Tai K, Ortiz CJ. Statistical indentation techniques for hydrated nanocomposites: concrete, bone, and shale. *J Am Ceram Soc* 2007;90:2677–92.